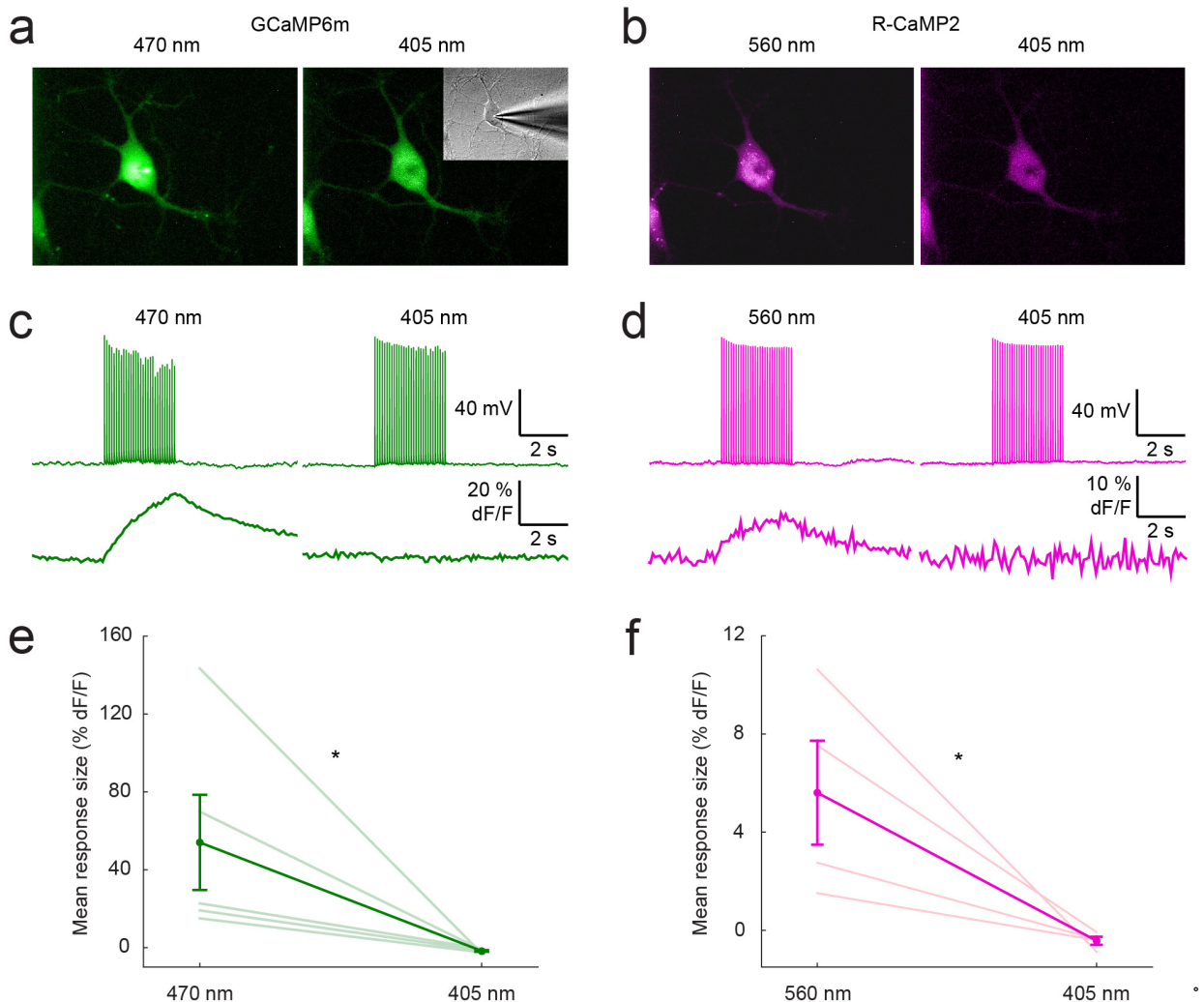


Supplementary Figure 1

Simultaneous camera and photoreceiver measurements of reward-related photometry signals in the VTA.

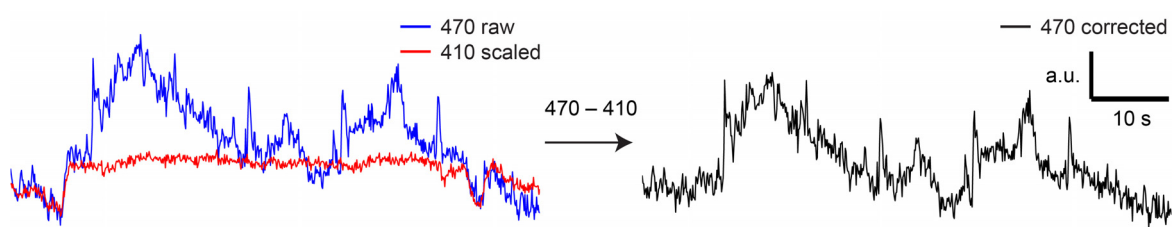
(a) Schematic of setup for simultaneous camera and photoreceiver measurements. Example images of the emission light from the fiber and the excitation spot are shown in the bottom left. Photoreceiver measurements were collected with a -3 dB rolloff frequency of 16 Hz, and camera measurements were collected at 32 Hz. The excitation LED was modulated at 448 Hz. (b) An example of a GCaMP6f Ca²⁺ transient measured from VTA-DA neurons in response to a single water reward is shown for both the camera and the photoreceiver (top). Six trials collected from the same animal are shown below for both the camera and photoreceiver. (c) The SNR of the camera measurements (14.03 ± 2.55) was significantly higher than that of the photoreceiver measurements (6.39 ± 0.70). Data plotted as mean \pm s.e.m. Asterisks indicate $p < 0.005$, Wilcoxon's signed-rank test, $n = 11$ trials from 2 mice. (d) There was no significant difference between the peak dF/F measured between the camera (8.98 ± 0.93 % dF/F) and photoreceiver (8.47 ± 0.79 % dF/F). Data plotted as mean \pm s.e.m. $p > 0.05$, Wilcoxon's signed-rank test, $n = 11$ trials from 2 mice.



Supplementary Figure 2

GECI fluorescence emission to Ca^{2+} -dependent and -independent wavelengths.

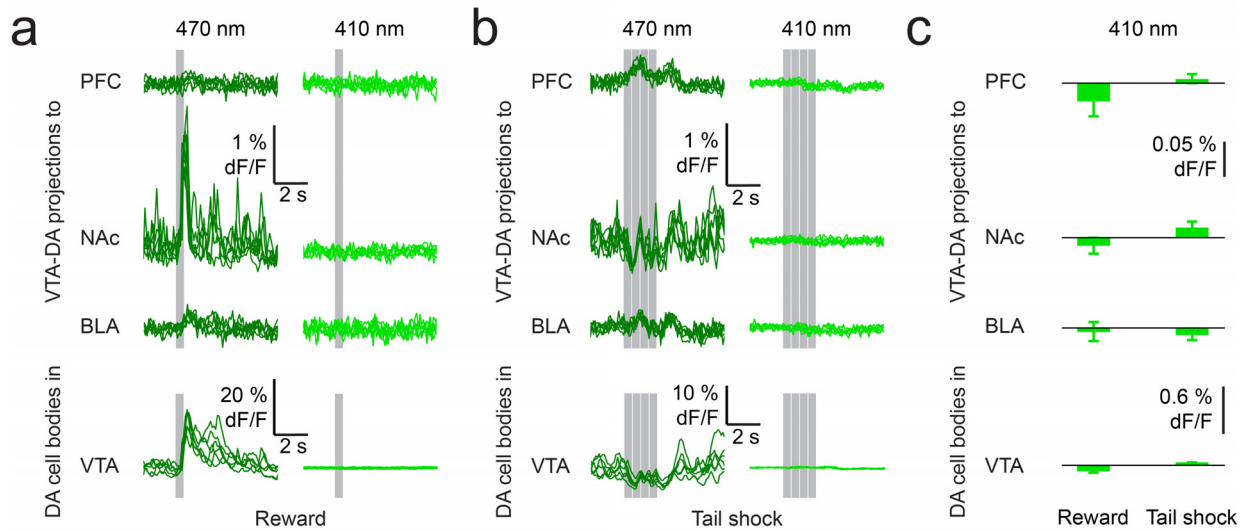
(**a-b**) Example images of a cultured neuron co-expressing GCaMP6m and R-CaMP2 taken with Ca^{2+} -dependent (470 nm and 560 nm) and isosbestic wavelengths (405 nm). Inset in (**a**) shows a DIC image of the recording pipette attached to the cell. (**c-d**) Simultaneously collected voltage (top) and fluorescence (bottom) recordings in response to 30 APs elicited by current injections. Ca^{2+} -dependent responses were measured with 470 and 560 nm light (left), while control responses were measured with 405 nm light (right). (**e-f**) Mean responses to 30 APs ($\text{dF/F}_{\text{stimulus}} - \text{dF/F}_{\text{baseline}}$). For both GCaMP6m and R-CaMP2, Ca^{2+} responses measured with 470 nm or 560 nm light were significantly greater than control fluorescence changes measured with 405 nm light (GCaMP6m response: $54.03 \pm 24\% \text{ dF/F}$, GCaMP6m control: $-1.67 \pm 0.43\% \text{ dF/F}$; R-CaMP2 response: $5.61 \pm 2.12\% \text{ dF/F}$, R-CaMP2 control: $-0.43 \pm 0.17\% \text{ dF/F}$). Asterisk indicates $p < 0.05$, Wilcoxon's rank-sum test, $n = 5$ cells for GCaMP6m and 4 cells for R-CaMP2.



Supplementary Figure 3

Correcting motion-related artifacts present in the 410-nm isosbestic wavelength.

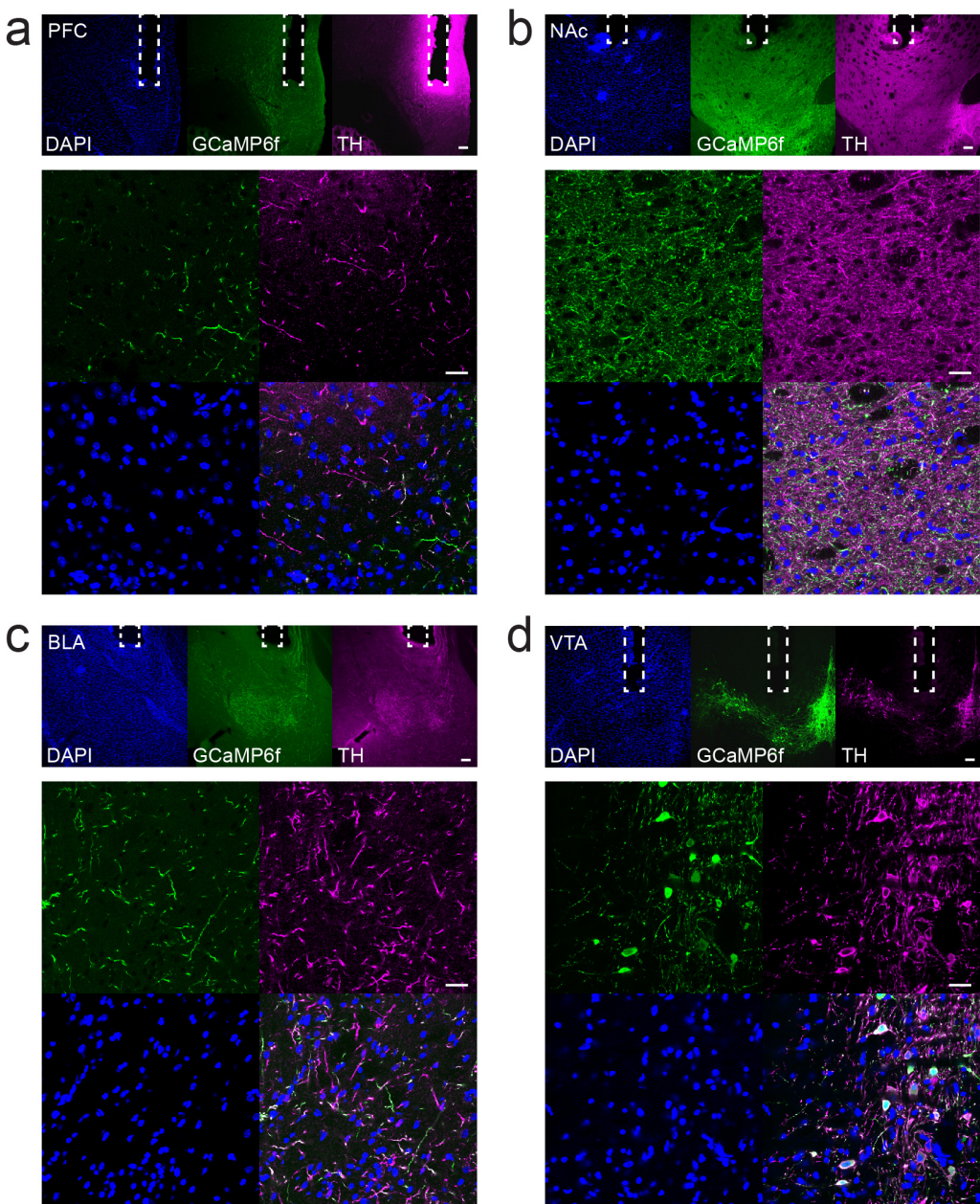
Example of simultaneously recorded GCaMP6 signals using 470 nm and 410 nm excitation *in vivo*. The 410 nm signal has been scaled using least-squares regression to minimize the difference between the 410 and 470 nm signal. We then subtracted the scaled 410 nm trace from the 470 nm trace to generate the corrected 470 nm signal.



Supplementary Figure 4

Individual traces of simultaneous four-fiber recordings of VTA-DA cell bodies and projections during reward and tail shock.

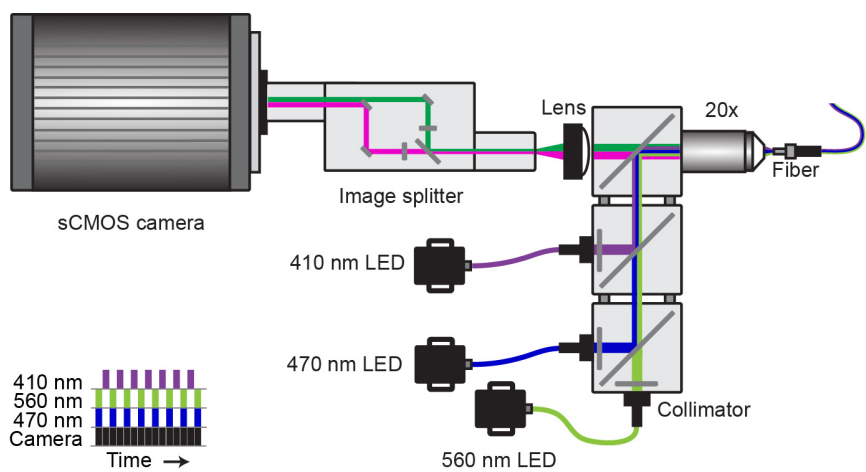
(a-b) Raw GCaMP6f responses to reward or tail shock shown for 6 individual trials. Dark green traces correspond to Ca²⁺-dependent GCaMP6f emission, and light green traces correspond to control traces (GCaMP6f emission with 410 nm light). **(c)** Mean control responses to reward or shock ($dF/F_{\text{stimulus}} - dF/F_{\text{baseline}}$). There were no significant responses in any brain region to reward or to shock ($p > 0.05$, Wilcoxon's signed-rank test, $n = 6$ trials from 1 mouse).



Supplementary Figure 5

Confirmation of fiber location and virus expression for four-fiber surgeries.

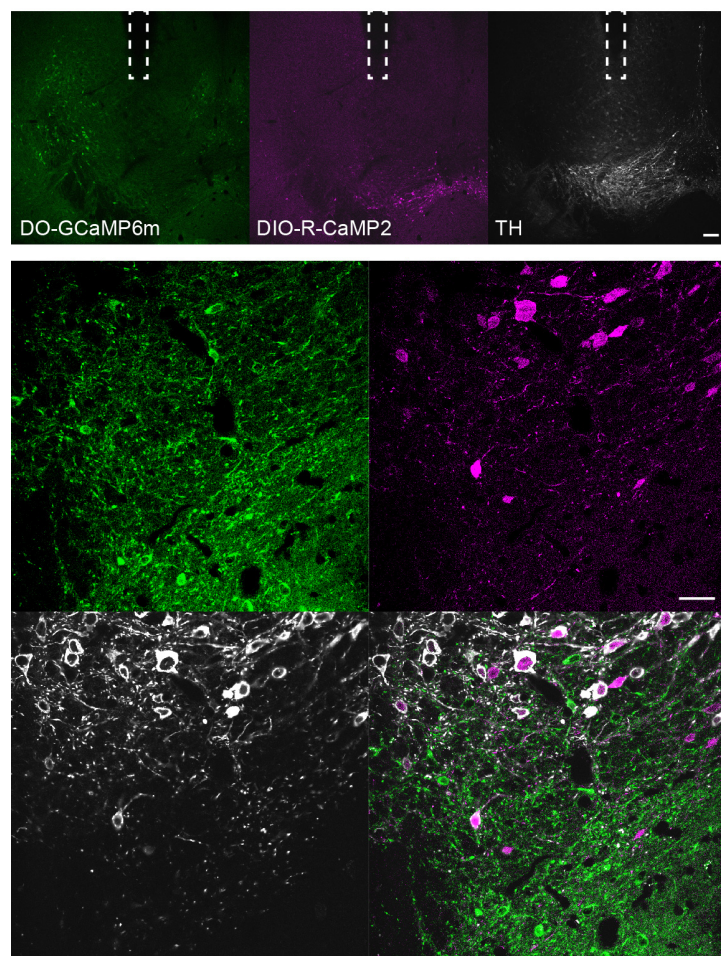
(a-d) Top: 10 \times magnification images of slices containing PFC, NAc, BLA, or VTA. Blue stain is for DAPI, green stain is for GCaMP6f, and magenta stain is for TH. Dashed white rectangles indicate fiber location. Scale bar indicates 100 μ m. Bottom: 63 \times magnification images of slices of same brain regions and staining. Bottom right image is a merge of all three channels. Scale bar indicates 25 μ m. Note that we observed very sparse GCaMP6f fibers localized to the amygdala regions surrounding the BLA that could also be contributing to the signal.



Supplementary Figure 6

Microscope configuration used for dual-color imaging.

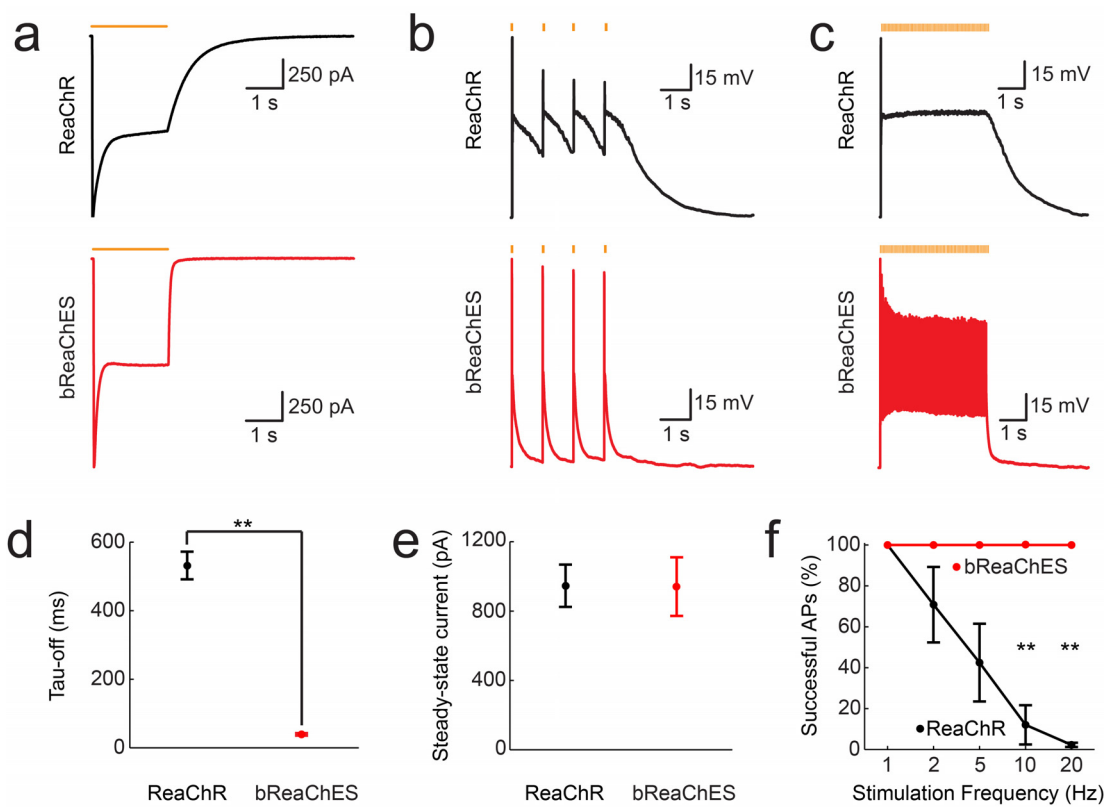
Schematic of setup for dual-color imaging. An image splitter was placed before the camera sensor, and an additional 560 nm LED was used to image R-CaMP2. The lower left diagram illustrates the time-division multiplexing strategy used to simultaneously image GCaMP6 and R-CaMP2 at both their Ca^{2+} -dependent and -independent wavelengths.



Supplementary Figure 7

Confirmation of fiber location and virus specificity for dual-color imaging.

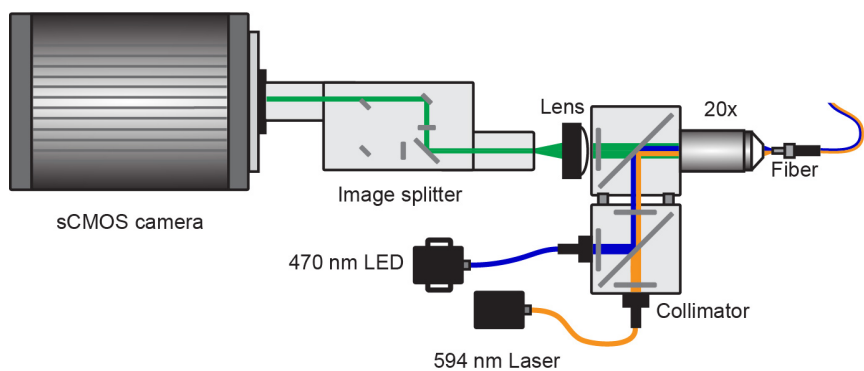
Top: 10 \times magnification images of a slice containing VTA. GCaMP6m fluorescence in VTA-non-DA neurons is shown in green, R-CaMP2 fluorescence in VTA-DA neurons is shown in magenta, and a TH stain is shown in white. Dashed white rectangle indicates fiber location. Scale bar indicates 100 μ m. Bottom: 63 \times magnification images of VTA slice with the same staining. Bottom right image is a merge of all three channels. Scale bar indicates 25 μ m.



Supplementary Figure 8

Characterization of novel bReaChES opsin.

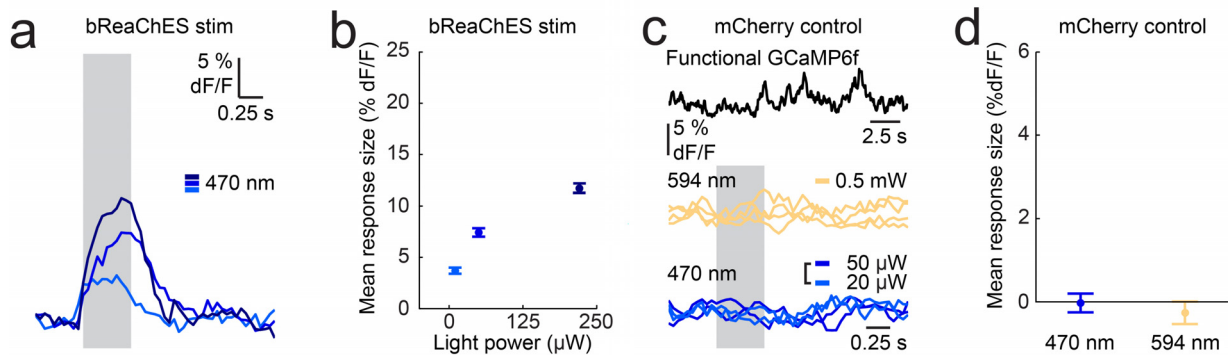
(a) Example of internal current elicited by a 4 s pulse of 590 nm light (orange) for neurons expressing ReaChR or bReaChES. (b) Voltage recordings showing 4 APs in response to 4, 5 ms pulses of 590 nm light (orange) delivered at 1 Hz to neurons expressing ReaChR or bReaChES. (c) Voltage recordings showing APs in response to 80, 5 ms pulses of 590 nm light (orange) delivered at 20 Hz to neurons expressing ReaChR or bReaChES. (d) The mean tau-off for bReaChES was significantly smaller than that of ReaChR (ReaChR: 531.83 ± 40.29 ms; bReaChES: 39.33 ± 3.69 ms). Asterisks indicate $p < 0.005$, Wilcoxon's rank-sum test, $n = 6$ cells. (e) There was no significant difference between steady-state current between ReaChR and bReaChES (ReaChR: 946.00 ± 121.97 pA; bReaChES: 941.17 ± 169.30 pA). $p > 0.05$, Wilcoxon's rank-sum test, $n = 6$ cells. (f) Percentage of APs successfully elicited by a 4 s train of 590 nm light pulses (5 ms pulse width) delivered at 1, 2, 5, 10, and 20 Hz to neurons expressing ReaChR or bReaChES. At 10 and 20 Hz, bReaChES stimulation elicited a significantly higher percentage of successful APs than ReaChR (ReaChR: $12.08 \pm 9.58\%$ at 10 Hz, $2.29 \pm 1.04\%$ at 20 Hz; bReaChES: $100 \pm 0\%$ at 10 and 20 Hz). Asterisks indicate $p < 0.005$, Wilcoxon's rank-sum test, $n = 6$ cells.



Supplementary Figure 9

Microscope configuration used for experiments involving simultaneous imaging and perturbation.

Schematic of setup for simultaneous imaging and perturbation experiments. The 560 nm LED was replaced with a 594 nm laser for optogenetic stimulation. For cross-stimulation measurements, the 594 nm laser was replaced with an additional 470 nm LED, and the dichroic combining the 470 nm and 594 nm light was replaced with a 50:50 beamsplitter.



Supplementary Figure 10

Controls for experiments involving simultaneous imaging and perturbation.

(a) Example GCaMP6f fluorescence traces in response to bReaChES cross-stimulation with 470 nm light (light to dark blue represents 10 μW , 50 μW , and 220 μW of power). (b) Summary of the mean GCaMP6f responses to bReaChES cross-stimulation with 470 nm light ($\text{dF/F}_{\text{stimulus}} - \text{dF/F}_{\text{baseline}}$). (c) Top: Example GCaMP6f fluorescence trace taken from a control mouse expressing mCherry instead of bReaChES to demonstrate that there is functional GCaMP6f present. Bottom: GCaMP6f fluorescence traces in response to 0.5 mW 594 nm stimulation pulses (orange), and to 20 or 50 μW 470 nm stimulation pulses (blue). (d) Mean GCaMP6f responses to light ($\text{dF/F}_{\text{stimulus}} - \text{dF/F}_{\text{baseline}}$) in the mCherry control mouse. There were no increases in GCaMP6f fluorescence with 470 nm or 594 nm stimulation light.

.

SUPPLEMENTARY NOTES

Supplementary Note 1. Simultaneous camera and photoreceiver lockin-in measurements.

To get a conservative estimate of how the sensitivity of the sCMOS camera without lock-in detection compares with the previous state-of-the-art technique employing lock-in detection, we conducted an experiment where we recorded the same Ca^{2+} -dependent fluorescence simultaneously with both techniques. To accomplish this, we modulated our excitation light source at 448 Hz and synchronized this with the lock-in amplifier configured with a -3 dB filter with 24 dB slope at 16 Hz (corresponding to a 10 ms time constant), consistent with the imaging parameters used in Gunaydin *et al.*¹ Modulating the excitation source at 448 Hz minimized both the presence of 60 Hz electrical noise in the photoreceiver, and beating artifacts from the modulated light in the camera. The emission from the fiber was equally split with a beamsplitter between the photoreceiver connected to the lock-in amplifier and the sCMOS camera. In order to match the 16 Hz bandwidth detection of the lock-in amplifier, we set the camera to acquire frames at 32 Hz (to Nyquist sample the desired 16 Hz bandwidth). Importantly, while the signal from the lock-in amplifier benefits from the demodulation of the 448 Hz carrier signal, we made no attempt to demodulate the signal recorded by the sCMOS camera though it would have been possible if we had sampled at a higher frame rate. Hence, the signal from the sCMOS camera is a conservative estimate of what would be measured with constant excitation without any modulation or lock-in detection.

Supplementary Note 2. Isosbestic excitation wavelength of GCaMP6 and R-CaMP2.

The published absorption spectrum of GCaMP3 and R-CaMP2 suggests that an isosbestic point between 405-420 nm exists where the absolute GCaMP or R-CaMP2 emission is independent of Ca^{2+} concentration. Previous studies using the AM esterase dye Fura-2², for example, have used fluorescence emission collected with the isosbestic excitation wavelength to measure Ca^{2+} -independent changes in fluorescence of the indicator. Thus by simultaneously measuring the GCaMP6 and R-CaMP2 fluorescence using the ~isosbestic 410 nm wavelength, we can record a reference signal that reports non- Ca^{2+} related fluorescence changes that could be contributing to the measured Ca^{2+} signals. In our paper we presented both the Ca^{2+} signals and control signals, and in some cases also normalized the Ca^{2+} signal by its corresponding control signal to better estimate neural activity-related changes in fluorescence. The ability to simultaneously record

both the Ca^{2+} -dependent signal and the 410 nm control signal allows us to identify artifacts that contaminate the signal in real-time, rather than in separate fluorophore-only cohorts.

Supplementary Note 3. Considerations when recording from multiple brain regions.

We note that when recording from multiple cell bodies across the brain, while the majority of the signal will likely be dominated by the local cell bodies, incoming axon terminals from other labeled brain regions could in principle contribute to the measured signal. However, as our projection data demonstrates, even the most robust projection (VTA-DA → NAc) produced signal that were at least an order of magnitude smaller than the local VTA-DA cell bodies. Future modifications to GECIs may improve the speed of cell body-restricted GCaMPs.

Supplementary Note 4. Generation of a novel bReaChES construct.

Recently a red-shifted excitatory opsin, ReaChR³, was published that exhibits large photocurrents capable of transcranial optogenetic stimulation. However, we found photocurrents expressing ReaChR were accompanied by a long tau-off, which hindered the ability to elicit APs at frequencies higher than 1 Hz. We introduced a mutation to the existing ReaChR to generate bReaChES⁴, which exhibits the same large photocurrents as ReaChR, but has a significantly short tau-off that allows APs to be driven 100 % reliably at up to 20 Hz.

Supplementary Note 5. Procedure for estimating cross-stimulation of bReaChES.

It is well known that the excitation spectrum of GCaMP6 and the excitation spectrum of red-shifted indicators such as C1V1 exhibit significant overlap⁵⁻⁷. As a result, a given choice of excitation wavelength for GCaMP6 will undoubtedly result in unwanted bReaChES cross-stimulation to some extent, and it is necessary to quantify this effect. To characterize the amount of cross-stimulation of bReaChES produced by the GCaMP6 excitation light, we applied additional pulses of 470 nm stimulation light at 20 Hz (10 pulses with 12.5 ms pulse width) while we imaged GCaMP6 with 470 nm light (20 Hz, 12.5 ms pulse width). As expected, with higher powers of the 470 nm blue excitation, we observed larger changes in GCaMP6 fluorescence likely due to cross-stimulation of bReaChES. As a comparison, we also measured the change in GCaMP6 fluorescence to interleaved pulse trains of 594 nm light at 20 Hz (10 pulses with 12.5 ms pulse width) intended to stimulate bReaChES, and to a water reward. This

protocol for characterizing the amount of cross-stimulation is a more explicit measure than those used in previous papers. Rickgauer *et al.*⁵ and Packer *et al.*⁶ characterized the amount of C1V1 cross-stimulation with 920 nm light by either increasing the two-photon laser power or increasing the scan speed to generate a curve of the resulting change in baseline GCaMP activity. Szabo *et al.*⁷ measured the amount of ChR2 cross-stimulation with 470 nm light by measuring the initial change in GCaMP6 fluorescence at the beginning of their recording. In particular we found that this last procedure for measuring cross-stimulation was insufficient as we observed no detectable change in GCaMP6 fluorescence at the start of our recording with low 5 μ W 470 nm imaging light, but could still detect small changes in fluorescence with our additional short pulses of 470 nm stimulation light.

Supplementary Note 6. System design, alignment, and calibration considerations.

First, a basic microscope consisting of the objective lens and tube lens was constructed, where the sCMOS camera was focused on the fiber(s) mounted at the working distance of the objective. Here, the objective and tube lens were chosen to set the magnification of the fibers onto the sensor, which determines the number of pixels on the camera that a given fiber tip is imaged onto. Note that the objective field of view and NA must be larger than the fiber size and NA. Given that the dominant noise source of the sCMOS camera is read noise, it is optimal, for a given quantity of emission photons, to sample them with as few sCMOS pixels as possible without saturating any pixels. However, for low light levels, photon shot noise may dominate the read noise, in which case it may be necessary to use more excitation light power to generate more emission photons, which may necessitate the use of more camera pixels to sample the emission without saturating. The excitation light sources were then added using dichroic mirrors between the tube lens and the objective. Similar to the tube lens of the camera, the focal length of the collimators for each excitation light source was chosen to set the magnification and NA to correctly fill the fiber(s). To align the relayed image of each excitation light source onto the previously aligned fiber(s), the position of the fiber(s) was annotated in the camera view and the excitation light sources were each positioned to be centered over the fiber(s). Finally, in the dual-color imaging experiments with the image splitter, the image splitter was simply attached to the camera and positioned until the now two images of the fiber(s) were in focus again. The synchronization of the light sources to the sCMOS camera was tested using a fluorescent slide.

The duty cycle and precise on-time of each light source was adjusted to accommodate the camera's rolling shutter and the off-slew-rate of each light source. This timing adjustment only had to be done once for each light source for each set of digital control waveforms.

SUPPLEMENTARY TABLES

Supplementary Table 1. Reproducibility of significant GCaMP6 responses to reward or tail shock with 470 nm light for four-fiber experiment.

Brain Region	Reward	Tail Shock
VTA-DA→PFC	n.s.	3 mice
VTA-DA→NAc	7 mice	4 mice
VTA-DA→BLA	3 mice	2 mice
VTA-DA	6 mice	5 mice

$p < 0.05$, Wilcoxon's signed-rank test, $n = 6\text{-}12$ trials for each mouse. $p > 0.05$ for control GCaMP6 responses with 410 nm light for all mice.

SUPPLEMENTARY REFERENCES

1. Gunaydin, L. A. *et al. Cell* **157**, 1535-1551 (2014).
2. Foehring, R. C., Zhang, X., Lee, J. C. & Callaway, J. C. *J. Neurophysiol.* **102**, 2326-2333 (2009).
3. Lin, J. Y. *et al. Nat. Neurosci.* **16**, 1499-1508 (2013).
4. Rajasethupathy, P. *et al. Nature* **526**, 653-659 (2015).
5. Rickgauer, J. P., Deisseroth, K. & Tank, D. W. *Nat. Neurosci.* **17**, 1816-1824 (2014).
6. Packer, A. M., Russell, L. E., Dalgleish, H. W. P. & Häusser, M. *Nat. Methods* **12**, 140-146 (2015).
7. Szabo, V. *et al. Neuron* **84**, 1157-1169 (2014).